MÖSSBAUER STUDIES OF CHEMICAL BONDING

By J. F. DUNCAN
(CHEMISTRY DEPARTMENT, VICTORIA UNIVERSITY OF WELLINGTON, NEW ZEALAND)
and R. M. GOLDING
(CHEMISTRY DIVISION, DEPARTMENT OF SCIENTIFIC AND INDUSTRIAL RESEARCH, WELLINGTON, NEW ZEALAND)

SPECTROSCOPY is the study of absorption and/or emission of electromagnetic radiation between two or more energy levels. In optical absorption spectroscopy, we examine transitions (*ca.* 30,000 cm.$^{-1}$) between the electronic ground state and the excited states; in infrared spectroscopy between vibrational ground and excited states (*ca.* 1000 cm.$^{-1}$); in electron spin resonance spectroscopy, between electron spin states arising from the interaction of the magnetic field with the electron (*ca.* 0·3 cm.$^{-1}$); and in nuclear magnetic resonance spectroscopy, between nuclear spin states arising from interaction of the magnetic field with the nucleus (*ca.* 0·002 cm.$^{-1}$). Mössbauer spectroscopy is simply a study of the absorption of electromagnetic radiation (γ-rays) between the nuclear ground and excited states (*ca.* 10^8 cm.$^{-1}$).

Since the first Mössbauer experiments in 1958,[1] physicists have used the principle in a variety of investigations, especially for studying atomic motions in solids.[2] However, it is only recently that chemists have realised the importance of Mössbauer spectroscopy for examining electronic configurations and the structures of chemical compounds. In this Review, we discuss only those features of Mössbauer spectroscopy pertinent to chemistry.

1. Fundamental Features

Mössbauer spectroscopy is the study of γ-ray absorption (or emission) between the ground and excited states (usually the first) of a specific type of nucleus. The energy difference between the ground and excited states of the transition involved is usually 10—100 kev (1 kev = 8·07 × 10^6 cm.$^{-1}$).

When an isolated atom emits a γ-ray, the total momentum of the system remains constant, *i.e.*, the recoil momentum of the atom is equal to the momentum of the γ-ray, E_0/c, where c is the velocity of light and E_0 the energy of the γ-ray when the decaying nucleus is at rest. Thus, for an emitted γ-ray,

$$E_\gamma = E_0\left(1 - \frac{v^2}{2c^2}\right), \quad (1)$$

and for an absorbed γ-ray,

$$E_\gamma' = E_0\left(1 + \frac{v^2}{2c^2}\right). \quad (2)$$

[1] Mössbauer, *Z. Physik.*, 1958, **151**, 124; *Naturwiss.*, 1958, **45**, 538.
[2] Boyle and Hall, *Proc. Phys. Soc.*, 1962, **25**, 441.

The recoil velocity, v, depends, in general, on the thermal motion of the nucleus, but when the decaying nucleus is bound in such a way that the recoil momentum is absorbed entirely by the lattice, the change in E_γ is negligible, and a γ-ray spectrum centred at E_0 is obtained (eqn. 1). A similar situation obtains when γ-ray absorption takes place (eqn. 2).

If we now mechanically move the emitter at a velocity v', the Doppler shift[3] in the energy of the emitted γ-ray is E_0v'/c, which corresponds, for instance, to $4{\cdot}8 \times 10^{-7}$ ev per cm./sec. velocity for the 14·4-kev γ-ray emitted in the decay of ^{57}Fe from the first exicted state to the ground state. Since the Doppler shift may be varied by altering the velocity of the source, E_γ may be adjusted until allowance has been made for the small difference in the energy level of the first excited state above the ground state in the source compared to that in the absorber (in a chemically different environment). Nuclear absorption of the γ-radiation will then occur.

2. Theoretical Aspects

As a consequence of the intrinsic nuclear spin, $I\hbar$ (or I in quantum units), the nucleus may interact with magnetic and electric fields in the molecule. These interactions may be represented by the spin-Hamiltonian operator:

$$\mathscr{H} = -\hbar\gamma H.I + P\,[\{3I_z^2 - I(I+1)\} + \frac{\eta}{2}\{I_+^2 + I_-^2\}]. \qquad (3)$$

Here, γ is the gyromagnetic ratio of the nucleus in a particular state with nuclear spin I; I_+ and I_- are step-up and step-down operators;[4] $P = e^2qQ(1-\gamma_\infty)/4I(2I-1)$, where eQ, the quadrupole moment of the nucleus, is non-zero when $I \geqslant 1$, eq is the electric-field gradient parallel to the z axis,[5] and $(1-\gamma_\infty)$ is Sternheimer's screening factor;[6] and η is the asymmetric parameter of the field-gradient tensor.

A magnetic field lifts the degeneracy of the nuclear states into the $(2I+1)$ Zeeman levels, the separations being determined by the magnetic- and electric-field interactions, for which $M_I = I, I-1, \ldots . -I+1, -I$. To illustrate the typical energy-level diagram so obtained, we can consider the ground ($I = \frac{1}{2}$) and first excited ($I = \frac{3}{2}$) states of the ^{57}Fe nucleus when the magnetic field is parallel to the z axis and the asymmetric parameter, η, is zero. The spin-Hamiltonian operator now becomes

$$\mathscr{H} = -\hbar\gamma H_z I_z + P\{3I_z^2 - I(I+1)\}. \qquad (4)$$

The energy-level diagram obtained for the ^{57}Fe nucleus, using the constants in Table 1, is shown in Fig. 1. The subscripts 'g' and 'e' refer to the ground

[3] See, for example, Jenkins and White, "Fundamentals of Optics," McGraw-Hill, New York, 1950.
[4] Griffith, "The Theory of Transition-Metal Ions," Cambridge University Press, Cambridge, 1961.
[5] See, for example, Das and Hahn, *Solid State Physics*, 1958, Suppl. 1.
[6] Sternheimer, *Phys. Rev.*, 1951, **84**, 244; *ibid.*, 1952, **86**, 316; *ibid.*, 1954, **95**, 736.

TABLE 1. *Nuclear properties of some Mössbauer nuclei.*

Nucleus	Natural abundance (%)	Nuclear spin		Gyromagnetic ratios	
		Ground state	First excited state	Ground state	First excited state
		I_g	I_e	γ_g	γ_e
^{57}Fe	2·25	$\frac{1}{2}$	$\frac{3}{2}$	+0·179	−0·102
^{119}Sn	8·68	$\frac{1}{2}$	$\frac{3}{2}$	−2·082	+0·448
^{166}Er	33·41	0	2	0	±1·21
^{197}Au	100	$\frac{3}{2}$	$\frac{1}{2}$	+0·0959	+0·76

$g_N\beta_N = \hbar\gamma = \mu/I$, where g_N is the nuclear Landé g factor, β_N the nuclear magneton γ the gyromagnetic ratio, and μ the magnetic moment

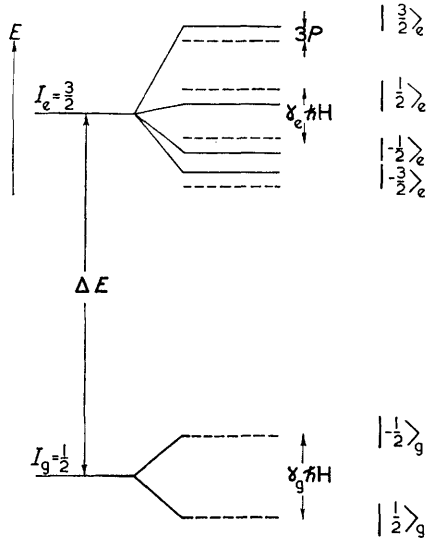

FIG. 1. *Energy-level diagram for the* ^{57}Fe *nucleus.* ΔE *is the energy separation of the ground and first excited states. The magnetic-field and the electric-field gradient inter-actions are indicated. (The subscripts 'g' and 'e' refer to the ground and first excited states, respectively.)*

and first excited states, respectively. Similar energy-level diagrams can be obtained for ^{119}Sn, ^{125}Te, ^{129}Xe, ^{169}Tm, and ^{171}Yb. Knowing the energy levels, we may next discuss the intensities of the hyperfine structure of the γ-ray absorption spectrum, *i.e.*, the transition probabilities between the Zeeman levels. These have been determined from the general theory of multipole radiation.[7] The angular intensity distribution, $I_M(\theta)$, for dipole radiation is

$$I_M(\theta) = \sum_m |\langle I_e\, 1\, M-m\, m | I_e\, 1\, I_g\, M\rangle|^2 \times \{1 + \tfrac{1}{4}(3m^2 - 2)(3\cos^2\theta - 1)\}. \quad (5)$$

Here, θ is measured about the axis of quantization, the Wigner coefficients $\langle I_e\, 1\, M-m\, m \mid I_e\, 1\, I_g\, M\rangle$ are known constants, and $m = 1, 0, -1$. In Table 2, the relative intensities from the ground to the first excited states, and the corresponding relative energies, for ^{57}Fe are given. When the

[7] Fagg and Hanna, *Rev. Mod. Phys.*, 1959, **31**, 711.

TABLE 2. *The relative energies and the relative intensities of transitions between the ground and the first excited states for* ^{57}Fe.

Excited state $\lvert M - m\rangle$	Ground state $\lvert M\rangle$	Relative energies	Relative intensities
$\pm\frac{3}{2}$	$\pm\frac{1}{2}$	$\mp\frac{\hbar H}{2}(3\gamma_e - \gamma_g) + 3P$	$\frac{3}{4}(\cos^2\theta + 1)$
$\pm\frac{1}{2}$	$\pm\frac{1}{2}$	$\mp\frac{\hbar H}{2}(\gamma_e - \gamma_g) - 3P$	$\sin^2\theta$
$\mp\frac{1}{2}$	$\pm\frac{1}{2}$	$\pm\frac{\hbar H}{2}(\gamma_e + \gamma_g) - 3P$	$\frac{1}{4}(\cos^2\theta + 1)$
$\mp\frac{3}{2}$	$\pm\frac{1}{2}$	$\pm\frac{\hbar H}{2}(3\gamma_e + \gamma_g) + 3P$	0

emitting nucleus interacts with magnetic and electric fields, the γ-ray absorption splits into a six-line spectrum. Provided that the absorber has a single-energy resonance, the emission spectrum will also be observed as six lines. The energy separations of these transitions depend on the magnitudes of the two interacting fields. Fig. 2 illustrates the relative separation of the six-line spectrum for various magnetic-field and electric-field gradient ratios which we have evaluated for the ^{57}Fe nucleus, taking $\gamma_e/\gamma_g = -0{\cdot}572$. The relative intensities of the six transitions are indicated. Fig. 2 shows that, when the effective magnetic field (H_z) is zero and only an electric-field gradient is present at the nucleus, the spectrum is a doublet. From eqns. 3 and 4 (or Fig. 2), the intensity ratio is

$$3(1 + \cos^2\theta) : (5 - 3\cos^2\theta).$$

In Mössbauer experiments with polycrystalline compounds, relative intensities are calculated by averaging over all angles of θ, the average values of $\sin^2\theta$ and $\cos^2\theta$ being $\frac{2}{3}$ and $\frac{1}{3}$, respectively. Consequently, the arms of the doublet, arising from the interaction of the electric-field gradient with the ^{57}Fe nucleus in a powdered sample of an iron compound, are of equal intensity. Deviations from equality are due to preferred orientations in the powders.[8]

When a magnetic field is present, either externally applied or inherent in the material, the intensities of the six γ-ray absorption (or emission) peaks for a powdered iron or iron complex are in the ratio 3:2:1:1:2:3, and if the nucleus is in a preferred orientation the relative intensities[9] are $3:\beta:1:1:\beta:3$, where $\beta = 4/(1 + 2\cot^2\theta)$ and $0 \leqslant \beta \leqslant 4$.

[8] Boyle, Bunbury, and Edwards, *Proc. Phys. Soc.*, 1962, **79**, 416.
[9] Preston, Hanna, and Heberle, *Phys. Rev.*, 1962, **128**, 2207.

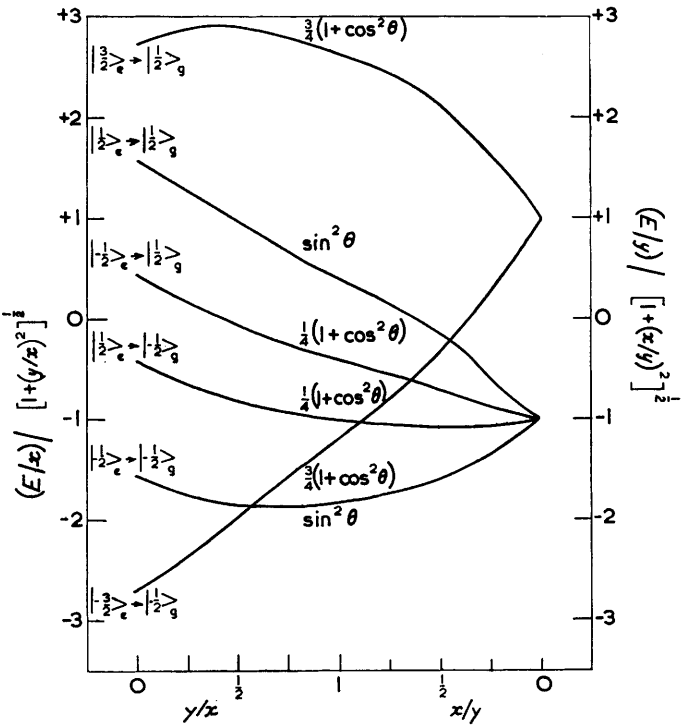

FIG. 2. *Separation of the six-line spectrum for the* ^{57}Fe *nucleus at different magnetic-field and electric-field gradient ratios:* $\gamma_e/\gamma_g = -0{\cdot}572$, $x = \gamma_g\hbar H/2$ and $y = 3P$.

2.1 Internal Magnetic Fields in Molecules.—Internal magnetic fields in atoms and molecules arise through the interaction of the *s* electrons with the nucleus; this is mathematically expressed in the spin-Hamiltonian by the Fermi contact term. In the usual symbolism:

$$H_z = \frac{8\pi}{3} g\mu |\psi_s(0)|^2 \langle S_z \rangle,$$

where the effective internal magnetic field at the nucleus, H_z, depends on the time-averaged value of the z component of the electron spin, $\langle S_z \rangle$. There is an additional term in the total spin-Hamiltonian contributing to the effective magnetic-field interaction with the nucleus, namely, that arising from the interactions between the electron and nuclear spins and the electron angular momentum. This, the dipolar term, is usually much smaller than the Fermi contact term.[10] If the electronic ground state of a

[10] Golding, *Mol. Phys.*, in the press.

typical transition-metal ion were truly represented by $(1s^2)$ $(2s^2)$ $(2p^6)$ $(3s^2)$ $(3p^6)$ $(3d^n)$ [*i.e.*, using the Aufbau principle], the total *s*-electron spin density at the nucleus would be zero. However, large effective magnetic fields have been observed in these atoms.[11] Sternheimer suggests[6] that the outer unpaired electrons polarise the core electrons to produce a finite *s*-electron spin density. We may relate this to observed Mössbauer spectra as follows.

The Aufbau principle implies that the wave functions of the two electrons in the same *s* shell have the same radial function and differ only in the electron spin, $+\frac{1}{2}$ or $-\frac{1}{2}$ (α or β). However, if there is an odd α-spin electron present, then it will experience different exchange interactions with the remaining α-spin electrons (including those in the core) from those with the β-spin electrons. Consequently, the α- and β-spin *s* electrons will have different radial functions, leading to a net *s*-electron spin density, $|\psi_\alpha(0)|^2 - |\psi_\beta(0)|^2$. Thus the electron spin density for closed *s*-electron shells is not necessarily zero. Abragam *et al.*[12] define a parameter

$$\chi = \frac{4\pi}{S} \sum_{s \text{ shells}} \{ |\psi_\alpha(0)|^2 - |\psi_\beta(0)|^2 \}, \qquad (6)$$

where S denotes the number of unpaired electrons. They showed that for the first transition-metal series, χ was approximately constant ($-$ 3 atomic units). This leads to an effective magnetic field, through the Fermi contact term, of -125 kgauss per unpaired $3d$ electron. Watson and Freeman[13] confirmed this constancy of χ from free-ion spin-polarised Hartree–Fock calculations. Thus, the magnetic field at the nucleus of a transition-metal compound is very large, being about -500 kgauss.

The value of χ is sensitive to the symmetry and nature of the ligands surrounding the transition-metal ion. For example, the calculated value of χ for the free Ni^{2+} ion is $-3{\cdot}94$[13], whereas for the Ni^{2+} ion in a cubic field it is $-3{\cdot}27$;[14] the experimental values for internal magnetic fields at the manganese nucleus in Mn^{2+} ion complexes depend on the ligand,[15] as shown in Table 3. The negative core polarisation is usually less than expected, but this can be explained by configurational mixing of the

TABLE 3. *The observed internal magnetic field at the manganese nucleus for several* Mn^{2+} *compounds.*

Ligand	H_2O	F^-	CO_2^{2-}	O^{2-}	S^{2-}	Se^{2-}	Te^{2-}
$\|H_z\|$ (kgauss)	695	695	665	570—640	490	460	420

[11] Hanna, Heberle, Littlejohn, Perlow, Preston, and Vincent. *Phys. Rev. Letters*, 1960, **4**, 177; Hanna, Meyer-Schutzmeister, Preston, and Vincent, *ibid.*, p. 513.
[12] Abragam, Horowitz, and Pryce, *Proc. Roy. Soc.*, 1955, *A*, **230**, 169.
[13] Watson and Freeman, *Phys. Rev.*, 1961, **123**, 2027.
[14] Watson and Freeman, *Phys. Rev.*, 1960, **120**, 1134.
[15] Van Wieringen, *Discuss. Faraday Soc.*, 1955, **19**, 118.

TABLE 4. *The magnetic field at the nuclei of Mössbauer atoms in magnetically aligned environments.*

Nucleus	Host	H_z (kgauss)	Ref.
^{57}Fe	Fe	−342	11, 16
^{57}Fe	Co	|312|	17
^{57}Fe	Ni	|280|	17
$^{57}Fe^{3+}$ (tetrahedral)	Y iron garnet	392	17, 18
$^{57}Fe^{3+}$ (octahedral)	Y iron garnet	474	17, 18
^{59}Co	Fe	300	19
^{61}Ni	Ni	−170	20
^{119}Sn	Fe	− 81	21
^{119}Sn	Co	−205	21
^{119}Sn	Ni	+185	21
^{198}Au	Fe	1460	22

$3d^n4s^x$ excited states[23] into the ground state, this effect giving a positive contribution to the effective magnetic field at the nucleus. It is clear that large magnetic fields are present at nuclei as a result of electronic interactions. In Table 4, we quote a few typical examples for different Mössbauer nuclei. The nuclear spin will couple with this field, but if the electron-spin–lattice relaxation time is shorter than the Larmor frequency of the nucleus, then the time-averaged value of the internal magnetic field affecting the nucleus is zero. This is often (but not always) the case when the Mössbauer atom is not in a magnetically aligned lattice (*e.g.*, for paramagnetic substances in the absence of external magnetic fields). Usually, for this internal magnetic field to be observed, the electronic structure of all the atoms must be spatially aligned, *e.g.*, in a ferromagnetic complex. The six-line spectrum which results has been used to determine effective internal magnetic fields at iron nuclei in various lattices (see Table 4). In a recent study of the Mössbauer spectra of Fe^{3+} in corundum (a non-magnetically aligned matrix) at 78°K,[23a] this characteristic hyperfine structure was observed, which implies that the spin relaxation time must be sufficiently long to present a stationary magnetic field at the iron nucleus. In some cases, the magnetic behaviour of a substance depends upon the temperature. For instance, the Mössbauer spectrum for iron at, or above, the Curie temperature (773°) is a single line, indicating no interaction between the nucleus and any magnetic-field or electric-field gradient.

[16] Nagle, Frauenfelder, Taylor, Cochran, and Matthias, *Phys. Rev. Letters*, 1960, **5**, 364.
[17] Wertheim, *Phys. Rev. Letters*, 1960, **4**, 403; *J. Appl. Phys.*, 1960, **32**, 110S.
[18] Alff and Wertheim, *Bull. Amer. Phys. Soc.*, 1960, **5**, 428.
[19] Dash, Taylor, Nagle, Craig, and Visscher, *Bull. Amer. Phys. Soc.*, 1961, **6**, 136.
[20] Wegener and Obenshain, *Z. Physik.*, 1961, **163**, 17.
[21] Boyle, Bunbury, and Edwards, *Phys. Rev. Letters*, 1960, **5**, 553; Boyle, Bunbury, Edwards, and Hall, *Proc. Phys. Soc.*, 1961, **77**, 129.
[22] Roberts and Thomson, *Phys. Rev.*, 1963, **129**, 664.
[23] Walker, Wertheim, and Jaccarino, *Phys. Rev. Letters*, 1961, **6**, 98.
[23a] Wertheim and Remeika, *Phys. Rev. Letters*, 1964, **10**, 14.

However, below the Curie temperature, the averaged internal magnetic field is not zero, and the spectrum has the characteristic six lines[9] with spacings dependent upon the magnetisation of the material.[16]

2.2 Electric-field Gradients at Nuclei.—Both the experimental quadrupole interaction, P, and the internal magnetic field can be determined by fitting the experimental results from a Mössbauer spectrum to the calculated relative energies, using energies similar to those shown in Table 2. For example, Kistner and Sunyar[24] found an internal magnetic field of 510 kgauss, and a small quadrupole interaction, in antiferromagnetic Fe_2O_3. However, in diamagnetic and paramagnetic compounds, only the quadrupole interaction need appear in the spin Hamiltonian (eqn. 3), since the averaged effective internal magnetic field is zero (see above). For ^{57}Fe complexes, this leads to doublet Mössbauer spectra with relative intensities as predicted in Fig. 2. The doublet energy separation, ΔE_Q, can be evaluated from eqn. 4 with $H_z = 0$. For the ^{57}Fe nucleus,

$$\Delta E_Q = 6P = \frac{e^2qQ\,(1 - \gamma_\infty)}{2I\,(2I - 1)}, \tag{7}$$

so that the term governing the variation of ΔE_Q, in compounds with the same Mössbauer nucleus, is the electric-field gradient (*eq*) at the nucleus.

The energy of Coulomb interaction between the electrons and the protons in an atom can be written as a set of multipole interactions.[25] The constant term gives rise to the central-field energy, and it is of no interest to us here. The dipolar term vanishes, leaving the third term, the electric quadrupole interaction. The next non-vanishing term is such that interactions from this and higher terms are very small, and we shall ignore them. If there is no mixing between the nuclear states, then the Hamiltonian representing the quadrupole interaction can be written as

$$\mathscr{H}_q = \frac{e^2Q\langle r^{-3}\rangle}{2I(2I-1)} \sum_\lambda \left\{ \frac{I(I+1)}{r_\lambda{}^3} - \frac{3(r_\lambda I)^2}{r_\lambda{}^5} \right\}, \tag{8}$$

where $\langle r^{-3}\rangle$ is the averaged value of r^{-3} and I is the nuclear spin. The distance between the λth electron and the nucleus is r_λ.[26]

If we have an l^n electronic configuration, then the Hamiltonian (8) may be written[27] as

$$\mathscr{H}_q = \pm \frac{e^2Q\langle r^{-3}\rangle S\xi}{I(2I-1)}\, \eta\{3(L.I)^2 + \tfrac{3}{2}(L.I) - L(L+1)I(I+1)\}. \tag{9}$$

Here

$$\xi = \frac{2l + 1 - 4S}{S(2l-1)(2l+3)(2L-1)}, \tag{10}$$

[24] Kistner and Sunyar, *Phys. Rev. Letters*, 1960, **4**, 412.
[25] Cohen and Reiff, *Solid State Physics*, 1957, **5**, 321.
[26] Casimir, see ref. 25.
[27] Bleaney and Stevens, *Reports Progr. Phys.*, 1953, **16**, 108.

$S = n/2$, and $L = \frac{n}{2}(2l + 1 - n)$. The positive sign in this equation is taken when the shell is less than half-filled, and the negative sign when the shell is more than half-filled.

For the d^5 case, Fe^{3+}, $l = 2$ and $n = 5$; thus $L = 0$ and, from the Hamiltonian (9), it follows that $\Delta E_Q = 0$. However, for the d^6 case, Fe^{2+}, $L = 2$, and thus ΔE_Q is finite. Therefore, ionic paramagnetic iron(III) complexes will give a single-peak Mössbauer spectrum, but ionic ferrous complexes will show a quadrupole splitting (see below). The relative order of magnitude of the quadrupole interactions expected for octahedral iron complexes can be derived simply from the symmetry and multiplicity of the four possible ground states for d^5 and d^6 configurations, by examining the appropriate Tanabe and Sugano[28] diagrams arising from the electrostatic and crystal-field interactions.[29]

The ground terms arising from the d^5 electronic configuration are $^6A_1$ for the high-spin (Fe^{3+}) and $^2T_2$ for the low-spin (Fe^{III}) complexes. The d^6 electronic configuration yields $^5T_2$ and $^1A_1$ ground terms for the high-spin (Fe^{2+}) and the low-spin (Fe^{II}) complexes, respectively. We would expect a zero electric-field gradient from a spherical ground state A, but not for non-spherical ground wavefunctions such as T_2. In the latter case, a greater spin multiplicity would produce a greater electric-field gradient. Hence we obtain a semi-quantitative diagram relating the quadrupole moments expected for the four types of octahedral iron complexes.

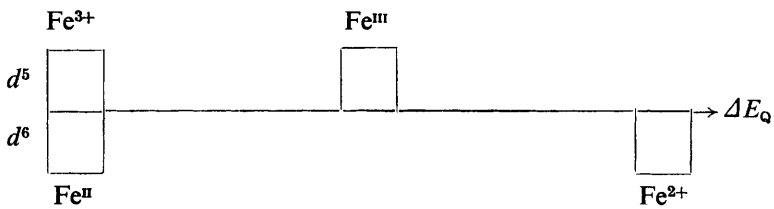

As discussed later, this type of semi-quantitative argument can be used to determine the type of iron complex in symmetrical octahedral fields. The field symmetry may, however, also be changed by altering the type of ligand in one or more of the co-ordination positions. For example, species like $[Fe(CN)_5NO]^{2-}$, $FeCl_2$, Fe(*o*-phenanthroline)$_2$(CN)$_2$, and $FeSO_4,7H_2O$ will all have different electric-field gradients because of the symmetry of the ligands nearest to the iron atom.

A relationship has recently been found[30] between the spin–spin parameter, D, obtained from electron spin resonance measurements, and the nuclear quadrupole splitting, ΔE_Q, obtained from Mössbauer experiments. This can be interpreted by means of the theory developed to explain the

[28] Tanabe and Sugano, *J. Phys. Soc. Japan*, 1954, **9**, 753.
[29] Duncan and Golding, I.U.P.A.C. meeting August, 1964.
[30] Nicholson and Burns, *Phys. Rev.*, 1963, **129**, 2490.

zero-field splitting in $3d^5$ ions. It has been known for some time that the ground state of ions such as Mn^{2+} and Fe^{3+} is split even in the absence of a magnetic field (zero-field splitting). This is usually represented by the spin-Hamiltonian

$$\mathscr{H} = D\{S_z^2 - \tfrac{1}{3} S(3 + 1)\} + E(S_x^2 - S_y^2), \quad (11)$$

where D and E are two experimentally determined parameters. Pryce[31] suggested that the splitting in Mn^{2+} arises from spin–spin coupling of unpaired electrons, and also from the electric-field gradient. Using these assumptions, Chakravarty[32] has derived expressions for D and E, namely,

$$D = -\tfrac{3}{2} g^2\beta^2 q\ (a_0^3/e)\langle DD\rangle \quad (12)$$

$$\text{and } E = -\tfrac{1}{2} g^2\beta^2\eta q(a_0^3/e)\langle EE\rangle \quad (13)$$

where g is the Landé splitting factor, β the Bohr magneton, and a_0 the Bohr radius. The parameters $\langle DD\rangle$ and $\langle EE\rangle$ were determined by using hydrogen-like wavefunctions. These expressions lead to the empirical linear relationship discussed by Nicholson and Burns:[30]

$$D = D_0 + keqQ/h, \quad (14)$$

in which k is an experimentally determined constant. Chakravarty[32] plotted the variation of D with eqQ/h for Fe^{3+} ions in several crystal lattices, using eqQ/h values determined by Nicholson and Burns.[30] This yields $D = 0$ when $q = 0$, which is expected when an ion is in a perfect cubic crystal-field. Any deviation from the spherical symmetry of this crystal field is reflected in the magnitudes of D, E, and q.

2.3 Isomeric or Chemical Shift.—In this section, we are interested in small variations in the energy differences between the ground and first excited states, arising from the environment of the nucleus.

Bodmer[33] showed that this energy difference, ΔE, is

$$\Delta E = \mathrm{F}(Z)|\psi_s(0)|^2\ \delta R_n/R_n \quad (15)$$

where F(Z) is a complex function of a number of nuclear parameters, including Z, the nuclear charge, R_n is the radius of the equivalent uniform charge distribution; δR_n is the difference between the radii of the ground and the first excited states; and $|\psi_s(0)|^2$ is the total s-electron density at the nucleus. ΔE is thus a measure of the s-electron density, which in turn depends upon the number of unpaired electrons and the nuclear environment. Mössbauer results are normally related to a reference emitter by defining the isomeric or chemical shift, δ, as

$$\delta = \mathrm{F}(Z)\ \delta R_n/R_n\{|\psi_s(0)|_A^2 - |\psi_s(0)|_E^2\}, \quad (16)$$

[31] Pryce, *Phys. Rev.*, 1950, **80**, 1107.
[32] Chakravarty, *J. Chem. Phys.*, 1963, **39**, 1004.
[33] Bodmer, *Nuclear Phys.*, 1961, **21**, 347.

where $|\psi_s(0)|^2_A$ and $|\psi_s(0)|^2_E$ refer to the *s*-electron densities of the absorber and the emitter, respectively. Hence, both the isomeric shift and the internal magnetic field, discussed previously, depend upon the total *s*-electron density at the nucleus.

The expected variation in isomeric shifts may be interpreted in a manner similar to that used in discussing ΔE_Q above. Since $|\psi_s(0)|^2_A$ is greatest when the number of unpaired electrons is largest, we expect the isomeric shift to decrease in the order $^6A_1$ .. $^1A_1$ and $^5T_2$ .. $^2T_2$. The *s*-electron density also depends markedly upon the environment of the Mössbauer nucleus (see Tables 3 and 4), and we can expect the effect of the α-induced polarisation of the *s* shells to be least for a symmetrical ground state. This is observed, and we can, therefore, qualitatively represent the variation in isomeric shift of octahedral iron complexes as follows:

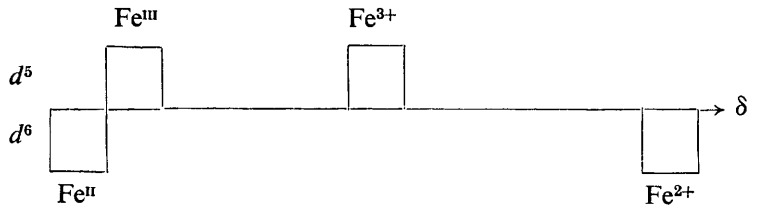

2.4 The $\delta/\Delta E_Q$ Correlation Diagram.—A diagram of δ plotted against ΔE_Q for the same Mössbauer nucleus has some interesting features.[34]

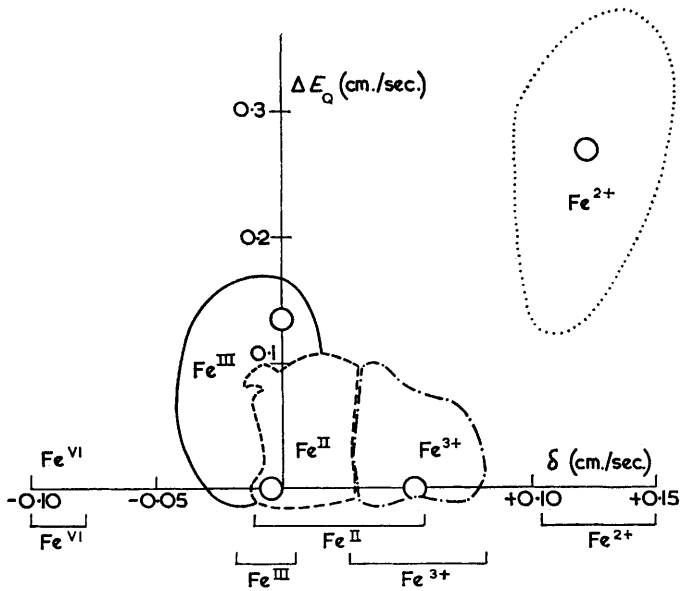

FIG. 3. *δ/ΔE_Q correlation diagram for a number of iron complexes. The circles indicate the approximate positions expected for iron complexes of octahedral symmetry.*

[34] Brady, Wigley and Duncan, *Rev. Pure Appl. Chem. (Australia)*, 1962, **12**, 165.

Fig. 3 shows the correlation diagram for a large number of iron complexes; the small circles indicate the positions expected for the octahedral iron complexes. The areas indicating Fe^{3+}, Fe^{III}, Fe^{2+}, Fe^{II} were obtained experimentally from results on about twenty different compounds of all types. With the aid of such a correlation diagram, it is possible to assign the electronic configuration and to study the influence of different ligands on the nucleus under examination.

2.5 Temperature-dependence.—In a previous section, we discussed the difference in Mössbauer spectra above and below the Curie temperature, due to the change in the magnetic properties of the material. Below the Curie temperature, an atom in a magnetically aligned environment usually shows hyperfine Zeeman splitting. The experimentally determined internal magnetic field (from the Zeeman splitting) in metals is found to be temperature-dependent; this corresponds closely to the temperature-dependence of the magnetisation.[16,35]

For there to be a change in the quadrupole splitting with temperature, it is necessary to have an electronic excited state close to the electronic ground state. This has been suggested[36] as an explanation of the marked temperature-dependence with Fe^{2+} salts such as $Fe(NH_4)_2(SO_4)_2,6H_2O$. However, in $3d$ iron complexes, the first excited electronic state is frequently well above the ground electronic state, and consequently a temperature-independent ΔE_Q term is obtained. This is not the case with the $4f$ rare-earth complexes. Here, spin–orbit coupling is very large, and the weak crystal-field interactions produce low-lying excited states leading to temperature-dependent quadrupole splitting. Mössbauer[37] observed such a temperature-dependent quadrupole splitting in thulium metal.

2.6 Other Correlations.—Any physical property dependent on the electronic or nuclear states will be related in some way to ΔE_Q and δ. Two examples must suffice.

The first is the linear relation between the magnetic susceptibility and ΔE_Q over a wide range of values for Fe^{3+} compounds.[38] Any deviation from the expected zero value of ΔE_Q for a d^5 Fe^{3+} ion must arise through an electric-field gradient at the nucleus, due to the ligands. In such a case, the magnetic-susceptibility variations in Fe^{3+} complexes must similarly depend upon the ligands.

A second example[39] is the linear relation between the proton magnetic resonance chemical shifts and the ^{57}Fe isomeric shifts for several cyclopentadienyl iron complexes.

Such correlations relate variations in the electronic ground and excited

[35] Meyer-Schutzmeister, Preston, and Hanna, *Phys. Rev.*, 1961, **122**, 1717.
[36] DeBenedetti, Lang, and Ingalls, Proc. 2nd Mössbauer Conf., Paris, Wiley, New York, 1961.
[37] Mössbauer, Proc. 2nd Mössbauer Conf., Paris, Wiley, New York, 1961.
[38] Brady, Duncan, and Mok, unpublished results.
[39] Herber, King, and Wertheim, *Inorg. Chem.*, 1964, **3**, 101.

states from compound to compound. An interpretation is to be sought in the *s*-electron density and the electric-field gradients in the atom. Since Mössbauer spectra enable these two quantities to be determined unequivocally at one place in the atom (the nucleus), the method illuminates, in a fundamental way, the interpretation of results determined by other methods.

3. Practical Aspects

In this section, we summarise those aspects likely to concern the reader who is considering work of this kind.

Two practical aspects of importance are (*a*) the nature of the necessary equipment, and (*b*) the number of suitable isotopes.

3.1 The Apparatus.—Spectra may be determined in a number of ways, the cost depending on the degree of sophistication employed.[34] Either scintillation or proportional counting methods may be used. The moving parts may be either electronically or mechanically driven. The latter is simpler, but the former allows errors in the movement to be eliminated by feedback methods. Both require special construction. The electronic method normally requires a wave-form generator, transducer (*e.g.*, high-fidelity loud-speaker) to drive the source, and associated components. The mechanical technique involves only workshop time and minor expenditure on materials, but good machining is essential to avoid loss of resonance intensity caused by vibrations.

Mössbauer spectra can be recorded in a variety of ways, depending on the method used for driving the source (or absorber). There are two general methods. The spectrum can be determined point by point, by moving the source at a constant velocity towards or away from the absorber. About ten minutes may be necessary to determine one point with sufficient accuracy, and therefore about five hours for a complete spectrum. Each point may be recorded independently either manually, or automatically by using a single scaling unit. The method is relatively cheap, but is subject to error from electronic drift. A second, more satisfactory, arrangement is to drive the source with a constant-acceleration cam (*ca.* 1 rev./min.). The output from the scintillation spectrometer is recorded against velocity. A convenient method is to employ a pulse-amplitude analyser with channel selection controlled by a potential related to the velocity at which the events are recorded. Anti-coincidence equipment, to reject unwanted pulses, may be useful. This reduces errors due to stray radiation, background fluctuations, etc.

3.2 Isotopes.—Even with ^{57}Fe, with which most work has so far been done, many possible applications of the Mössbauer effect in chemistry remain to be studied. However, there are a number of other isotopes which can be used; the situation is rather similar to that for nuclear magnetic resonance spectroscopy. About eighty isotopes which may be suitable have

been listed,[2,40] but not all have been shown experimentally to exhibit the effect.[41] Only ^{119}Sn and ^{57}Fe have been used for any systematic chemical work. In some cases, it has been asserted that low temperatures are essen-

TABLE 5. *Some suitable Mössbauer nuclei.*

Mössbauer nucleus	Decay scheme	Resonant energy (kev)	Chemical features	Ref.
^{57}Fe	^{57}Co→^{57}Fe (270 day)	14·4	*Source:* ^{57}Co in copper, stainless steel. *Absorbers:* numerous chemical compounds over a wide range of temperatures.	34
^{119}Sn	^{119}Sn*→^{119}Sn (250 day)	23·8	*Source:* in SnO_2. *Absorbers:* numerous chemical compounds over a wide range of temperatures.	47, 48, 49, 50, 51, 52, 53
^{125}Te	^{125}Te*→^{125}Te (58 day)	35	*Source:* ^{125}Sb in copper. *Absorbers:* MnTe, CrTe, α-TeO_2.	42, 43
^{129}I	^{129}Te→^{129}I (70 min.)	26·8	*Source:* ^{129}Te in ZnTe. *Absorbers:* iodides, iodates enriched with ^{129}I. Both source and absorber cooled in liquid nitrogen.	44, 45, 53*a*
^{129}Xe	^{129}I→^{129}Xe ($1{\cdot}6 \times 10^7$ yr.)	79	*Source:* in NaI, $NaIO_3$. *Absorber:* clathrate compounds, XeF_2, XeF_4.	46

[40] Frauenfelder, "The Mössbauer Effect," Benjamin, New York, 1962.
[41] Wertheim, *Science*, 1964, **144**, 253.
[42] Hien, Shapiro, and Shpinel', *Soviet Phys. JETP*, 1962, **15**, 489 (*Zhur. eksp. teor. Fiz.*, 1962, **42**, 703).
[43] Shikazono, *J. Phys. Soc. Japan*, 1963, **18**, 925.
[44] de Waard, de Pasquali, and Hafemeister, *Phys. Rev. Letters*, 1963, **5**, 217.
[45] de Waard, Garrell, and Hafemeister, *Phys. Rev. Letters*, 1962, **3**, 59.
[46] Jha, Segnan, and Lang, *Phys. Rev.*, 1962, **128**, 1160.
[47] Bryukhanov, Delyagin, Opalenko, and Shpinel', *Soviet Phys. JETP*, 1963, **16**, 310 (*Zhur. eksp. teor. Fiz.*, 1962, **43**, 432).
[48] Bryukhanov, Gol'danskii, Delyagin, Korytko, Makarov, Suzdalev, and Shpinel', *Soviet Phys. JETP*, 1963, **16**, 321 (*Zhur. eksp. teor. Fiz.*, 1962, **43**, 448).
[49] Aleksandrov, Delyagin, Mitrofanov, Polak, and Shpinel', *Soviet Phys. JETP*, 1963, **16**, 879 (*Zhur. eksp. teor. Fiz.*, 1962, **43**, 1242).
[50] Aleksevskii, Hien, Shapiro, and Shpinel, *Soviet Phys. JETP*, 1963, **16**, 559 (*Zhur. eksp. teor. Fiz.*, 1962, **43**, 790).
[51] Bryukhanov, Gol'danskii, Delyagin, Makarov, and Shpinel', *Soviet Phys. JETP*, 1962, **14**, 443 (*Zhur. eksp. teor. Fiz.*, 1962, **42**, 637).
[52] Boyle, Bunbury, and Edwards, *Proc. Phys. Soc.*, 1962, **79**, 416.
[53] Shpinel', Bryukhanov, and Delyagin, *Soviet Phys. JETP*, 1962, **14**, 1256 (*Zhur. eksp. teor. Fiz.*, 1961, **41**, 1767).
[53*a*] Perlow and Perlow, *Rev. Mod. Phys.*, 1964, **36**, 353.

TABLE 5.—*continued*

Mössbauer nucleus	Decay scheme	Resonant energy (kev)	Chemical features	Ref.
^{151}Eu	$^{151}Gd \rightarrow ^{151}Eu$ (140 day)	21·7	*Source:* in Nd_2O_3, Eu_2O_3. *Absorber:* Eu_2O_3.	54, 55
^{161}Dy	$^{161}Dy^* \rightarrow ^{161}Dy$ (7·2 day)	26	*Source:* Gd_2O_3. *Absorber:* Dy_2O_3.	56
^{166}Er	$^{166}Ho \rightarrow ^{166}Er$ (27 hr.)	80·7	*Source:* $HoAl_2$. *Absorbers:* Fe_2Er, Er, $ErFe_3Mn$, Er_2O_3.	56*a*
^{197}Au	$^{197}Pt \rightarrow ^{197}Au$ (18 hr.)	77	*Source:* enriched Pt foil. *Absorber:* Au, Au in Fe.	22

tial for observing the effect, but since the efficiency of recoilless productions and absorption of γ-radiation depends on the chemical form of the host material, this statement is not generally true. In Table 5, the relevant data are given for the principal isotopes with which the Mössbauer effect has been studied.

3.3 Other Experimental Features.—An important feature is the prevention of loss in the resonant γ-ray energy by nuclear recoil. This is usually accomplished by incorporating the radioactive atom in an ionic lattice, so that the whole of the source must recoil for each emission. It is, however, not satisfactory to choose just any ionic lattice for incorporating the radioactive material, since atomic vibrations of the emitting atom, which vary from one compound to another, can change the γ-ray energy sufficiently to preclude resonance. The more tightly bound the radioactive atom is (the higher the vibration frequency and the lower the vibration amplitude), the greater the resonance intensity. Careful source preparation is therefore essential. Fortunately, several methods for preparing satisfactory sources have already been given.[34] The same considerations, however, also apply to the absorber. Very poor resonances invariably result from poor absorber preparations, so that material which easily decomposes, or which cannot be easily purified, should not be used.

Another way of reducing the effect of nuclear vibration is to lower the temperature. This may, of course, alter the chemical environment, owing to phase changes and changes in the electronic ground state. But even if it does not, δ and ΔE_Q may be temperature-dependent. However, these temperature-dependent variations are small and well-known, so that lowering the temperature is a useful method of improving the detection of

[54] Shirley, Kaplan, Grant, and Keller, *Phys. Rev.*, 1962, **127**, 2097.
[55] Delyagin, Shpinel', and Bryukhanov, *Soviet Phys. JETP*, 1962, **14**, 959 (*Zhur. eksp. teor. Fiz.*, 1961, **41**, 1347).
[56] Sklyarevskii, Samoilov, and Stepanov, *Soviet Phys. JETP*, 1963, **16**, 1316 (*Zhur. eksp. teor. Fiz.*, 1961, **40**, 1874).
[56*a*] Cohen and Wernick, *Phys. Rev.*, 1964, **134**, B503.

γ-ray absorption. This is often done by using a foam-plastic vessel in which to keep the refrigerant.

3.4 Experimental Mössbauer Spectra.—The experimental features of a Mössbauer spectrum are quite simple. Figs. 4 and 5 show two typical Mössbauer spectra. The γ-ray absorption intensity is recorded against the Doppler-shift velocity (cm./sec.). Since the Doppler-shift energy is E_0v'/c (Section 1), this can be converted into the usual energy units by remembering that, for ^{57}Fe, 1 cm./sec. = 0·00388 cm.$^{-1}$. The spectrum is recorded in a pulse-amplitude analyser until several-thousand γ-ray quanta have been detected. To record a spectrum over a period of a few hours, therefore, requires a source of about 2 millicuries.

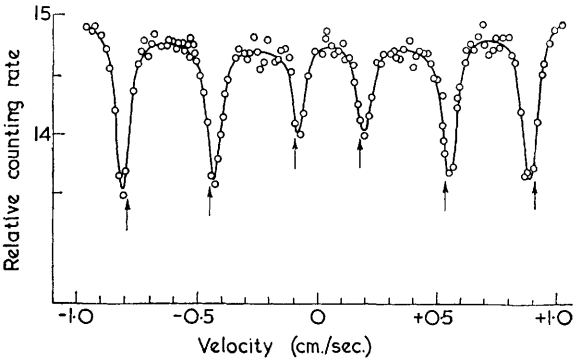

FIG. 4. *The Mössbauer spectrum for* ^{57}Fe *in antiferromagnetic* Fe_2O_3.[24] *The positions of the six hyperfine lines—intensity ratio* 3:2:1:1:2:3*—depend on the magnetic-field and electric-field gradient interactions. The arrows indicate the positions of the six lines if the electric-field gradient interaction were zero.*

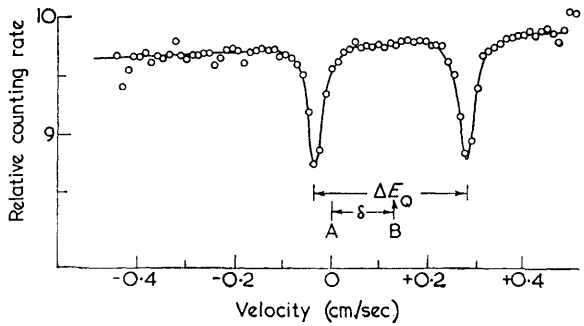

FIG. 5. *The Mössbauer spectrum of iron*(II) *sulphate:* ΔE_Q *is the quadrupole splitting;* δ *is the isomeric (or chemical) shift; and* A *and* B *refer to the energy of the stainless-steel single-line* γ*-ray emission and the centre of the iron*(II) *sulphate spectrum, respectively.*

The Mössbauer spectrum for ^{57}Fe in antiferromagnetic Fe_2O_3[24] (Fig. 4) shows the six hyperfine lines arising from the magnetic-field interaction (Section 2.1). When the effective magnetic field is zero, only the quadrupole interaction is observed; this is shown in Fig. 5, the Mössbauer spectrum of iron(II) sulphate. The quadrupole splitting, ΔE_Q, is, in this case, 0·320 cm./sec. ($\equiv$ 0·00124 cm.$^{-1}$). The isomeric shift, δ, the difference between the energy of the stainless-steel single-line γ-ray emission (A) and the centre of the iron(II) sulphate spectrum (B). Here, δ = 0·131 cm./sec. ($\equiv$ 5·08 $\times$ 10^{-4} cm.$^{-1}$). The magnetic-field and quadrupole interactions, and the isomeric shift, can thus readily be evaluated from a Mössbauer spectrum. In general, Mössbauer spectra are never more complicated than these, unless two or more species are present to give overlapping spectra.

4. Chemical Applications

In this Section, we discuss some illustrative examples of typical chemical problems. We have made no attempt to discuss the large number of compounds which have been studied (see earlier Reviews).[2,34,57] Table 6 gives some recent examples of the use of the Mössbauer effect.

4.1 Magnetic Fields in Alloys.—Included in Table 6 are several cases where chemical interest is centred on the source. This technique has been widely used in studying the magnetic fields of binary metallic compounds and alloys (Table 4). Both the magnitude and the sign of the internal magnetic field can readily be found in this way. The internal magnetic field at a nucleus may be either increased or decreased by an externally applied magnetic field. By convention, the internal magnetic field in the first case is taken as negative, and in the second case as positive. We have assumed here that the internal magnetic field is not affected appreciably by the domain magnetization. Nuclear magnetic resonance studies yield more accurate measurements of internal magnetic fields at nuclei, but, normally, the resonance is so broad that it is difficult to detect without prior knowledge of its position.

4.2 Structure of Compounds.—In the complex ferrocyanides, Prussian Blue, Turnbull's Blue, and Berlin Green, it has been shown[58] that, in all three cases, the cation and the anion are in the oxidized and reduced states, respectively, and that the compound prepared by precipitation from iron(III) sulphate and potassium cyanoferrate(II) is identical with that prepared from iron(II) sulphate and potassium cyanoferrate(II).

In the SnX_4 series of compounds, a linear relationship between the isomeric shift and both the electronegativity of the X atom and the degree

[57] Fluck, Kerler, and Neuwith, *Angew. Chem.*, 1963, **2**, 277.
[58] Duncan and Wigley, *J.*, 1963, 1120.

TABLE 6. *Recent examples of the use of the Mössbauer effect in chemical work.*

Source	Absorber	Type of work	Ref.
$^{57}Fe/^{57}Co$ in a single crystal of NaI.	Stainless steel.	Change in ΔE_Q observed for different orientations. Positive-hole vacancies and substitutional incorporation.	69
$^{57}Fe/^{57}Co$ in silicon and germanium.	^{57}Fe-enriched $K_4[Fe(CN)_6]$.	No difference between *n*- and *p*-types. Asymmetric positions for Fe^0 and Fe^{-1} in Ge lattice. Fe is electrically inactive.	62
$^{57}Fe/^{57}Co$ in stainless steel, and ^{119}Sn in SnO_2.	$FeSn_2$ as powder on beryllium disc.	Internal magnetic field below Curie point measured, and effect of this on ^{119}Sn resonances determined.	60
$^{57}Fe/^{57}Co$ in stainless steel.	Oriented FeF_2.	Internal magnetic field in antiferromagnetic state measured.	64
$^{57}Fe/^{57}Co$ in copper.	Glasses of $Na_2O,3SiO_2$ with Fe_2O_3 incorporated. $Fe(PO_3)_3$ crystals.	Magnetic hyperfine splitting in absence of external field, resulting from long electron-relaxation time. Antiferromagnetic below 10°K.	68
$^{57}Fe/^{57}Co$ in metallic chromium.	Ferrocene-type compounds.	Bonding of iron atom not affected by ring substitution.	65
$^{57}Fe/^{57}Co$ in metallic chromium.	$Fe(CO)_5$ and related compounds.	Results for $Fe(CO)_5$ and $Fe_2(CO)_9$ agree with trigonal bipyramid and 333 structures, respectively. $Fe_3(CO)_{12}$ probably is 3333 structure, and is not trigonal as *X*-ray results suggest. $Fe(CO)_4I_2$ is low spin.	63
$^{57}Fe/^{57}Co$ in metallic chromium.	$C_8H_8Fe_2(CO)_6$ $C_8H_8Fe(CO)_3$	Data indicate complete covalent bonding between iron atom and π-electron distribution of cyclo-octatetraene ring system.	66
$^{57}Fe/^{57}Co$ in stainless steel.	K_2FeO_4	Results interpreted in terms of d^3s hybridisation.	67
^{119}Sn in ^{118}Sn-enriched SnO_2.	Single-crystals of white tin cut along various crystal planes.	Large anisotropy studied for various orientations and temperature-dependence.	50

TABLE 6.—*continued*

Source	Absorber	Type of work	Ref.
^{119}Sn in SnO_2.	SnO_2, SnO, Sn, $Sn(NO_3)_2$.	Resonance intensity measurement and dependence of ΔE_Q on temperature.	55
^{119}Sn in SnO_2.	Tin-organic polymers.	Investigation of tin–carbon bonding.	51
^{119}Sn in SnO_2.	$(C_4H_9)_2SnX_2$ and related compounds.	ΔE_Q and δ vary with electronegativity of X.	49
$^{125}Te/^{125}Sb$ in copper or iron.	TeO_2, MnTe, CrTe.	Determination of internal field and nuclear moment.	68*a*
$^{131}I/^{131}Xe$ in NaI. $^{129}I/^{129}Xe$ in NaI, or $Na^{129}IO_3$, or $^{129}I_2$.	$^{131}XeF_4$ ^{129}Xe clathrate.	Study of Xe compounds such as XeO_3.	53*a*
$^{151}Eu/^{151}Gd$ in ^{151}Eu-enriched Eu_2O_3.	$Eu(EtHSO_4)_3$	ΔE_Q suggests mixing of $5p^56p^1$ ($^1D_2$) and $5p^6$ ($^1S_0$) states.	61
$^{197}Au/^{197}Pt$ in 19 metals and semiconductors at 4·2°K.	Gold	ΔE_Q correlated with electronegativity differences between host metal and gold.	59

[59] Barrett, Grant, Kaplan, Keller, and Shirley, *J. Chem. Phys.*, 1963, **39**, 1035.
[60] Nikolaev, Shcherbina, and Karchevskii, *Zhur. eksp. teor. Fiz.*, 1963, **44**, 775.
[61] Judd, Lovejoy, and Shirley, *Phys. Rev.*, 1962, **128**, 1733.
[62] Norem and Wertheim, *J. Phys. and Chem. Solids*, 1962, **23**, 1111.
[63] Herber, Kingston, and Wertheim, *Inorg. Chem.*, 1963, **2**, 153.
[64] Wertheim, *Phys. Rev.*, 1961, **121**, 63.
[65] Wertheim and Herber, *J, Chem. Phys.*, 1963, **38**, 2106.
[66] Wertheim and Herber, *J. Amer. Chem. Soc.*, 1962, **84**, 2274.
[67] Wertheim and Herber, *J. Chem. Phys.*, 1962, **36**, 2497.
[68] Kurkjian and Buchanan, *Phys. and Chem. Glasses*, 1964, **5**, 63.
[68*a*] Shikazano, *J. Phys. Soc. Japan*, 1963, **18**, 925.
[69] Mullen, *Phys. Rev.*, 1963, **131**, 1410; 1415.

of ionisation of the bond has been found.[70] Such a graph gives insight into the type of bonding in similar tin compounds. Any quadrupole splitting observed in these compounds would indicate a deviation from tetrahedral symmetry. For instance, the quadrupole splitting in SnF_4 has been attributed[71] to a polymeric structure in which each tin atom is bound to six fluorine atoms, two of which have no additional bonds while four form bridge bonds between the tin atoms.

4.3 Gas-phase Adsorption and Surface Reactions.—Mössbauer spectroscopy is also applicable to the study of solid-surface phenomena, such as gas-phase adsorption, and to surface reactions in liquid solutions. Little work of this type has so far been reported. The potentialities of the method can be illustrated by the adsorption of cobalt(II) ion on precipitates of cobalt(II) and iron(II) oxalates.[72] One would expect cobalt(II) to be adsorbed on the surface sites of these precipitates in such a way that the environment of the anions is asymmetric and quite different from that due to cations in the body of the solid. Experimentally, however, the shape of the Mössbauer spectrum, using such a source with a stainless-steel absorber, is identical, within experimental error, with that obtained with a copper-backed source and an iron(II) oxalate absorber. It is also very similar to that obtained with a cobalt(II) oxalate adsorbate; it is not affected by the length of time the precipitate is allowed to stand in contact with the active supernatant liquid; and is indistinguishable from spectra obtained when the precipitate is formed in the presence of radioactive material (*i.e.*, the ^{57}Fe was formed by decay from the ^{57}Co in lattice sites). From these results, two conclusions may be drawn. First, the environments of iron atoms in cobalt(II) and iron(II) oxalates are very similar. This implies that the crystalline structures are similar, which is not unreasonable in view of the similar ionic radii of the Co^{2+} and the Fe^{2+} ions. Secondly, the environment of surface-adsorbed ions is similar to that of ions within the lattice.

4.4 Single-crystal Studies.—The majority of Mössbauer spectra have been obtained from microcrystalline powders, which give only averaged spectra. Consequently, information is lost. By using a single crystal, we may observe the γ-ray absorption in different crystal orientations. It has been shown (Section 2) that, in paramagnetic iron complexes, the quadrupole-split doublet in the γ-ray absorption spectrum has an intensity ratio of $3(1 + \cos^2\theta):(5 - 3\cos^2\theta)$, where θ is the angle between the electric-field gradient and the γ-ray direction. Hence, from the ratio of the intensities of the doublet lines, the direction of the electric-field gradient in the single crystal can be determined. We have recently used this technique to determine the electric-field gradient in sodium nitroprusside single crystals.[73]

[70] Gol'danskii, Atomic Energy Review, vol. 1, No. 4, p. 3, International Atomic Energy Agency, Vienna, 1963.
[71] Khaiduk, see ref. 70.
[72] Brady and Duncan, *J.*, 1964, 653.
[73] Duncan and Golding, unpublished results.

Single-crystal studies can sometimes readily reveal the presence of more than a single site in the lattice. For example, Alff and Wertheim,[74] using a single crystal of yttrium iron garnet, have shown that there are three non-equivalent sites (one octahedral and two tetrahedral) for the ^{57}Fe atoms in the structure.

4.5 Electronic Configurations.—From the internal magnetic field or the isomeric shift, δ, we can evaluate the *s*-electron density at the nucleus from the nucleus–electron interaction represented by the Fermi contact term in the spin Hamiltonian (eqn. 5). This term also accounts for the isotropic hyperfine interaction in electron spin resonance spectroscopy[12] and the magnitudes of temperature-dependent shifts in nuclear magnetic resonance spectra of paramagnetic complexes.[10] Such measurements are therefore important in order to test the validity of an electronic configuration for a molecule. For instance, the naïve Aufbau principle implies a zero Fermi contact interaction. However, we deduce from experiments that this is not the case. The Fermi term probably arises in three ways,[4] namely, (i) from mixing of excited electronic states containing unpaired *s*-electrons with the ground state, (ii) by a spin-polarisation effect due to different spin-exchange interactions, and (iii) by ligand-field mixing of the appropriate electronic configuration with the ground state.

These important features of molecular electronic configuration can readily be investigated by means of Mössbauer spectroscopy. This new technique in chemistry thus provides ways in which basic ideas about molecular structure can be investigated, and is a valuable extension to the general field of spectroscopy.

This work is supported, at the Victoria University of Wellington, by the United States Air Force.

[74] Alff and Wertheim, *Phys. Rev.*, 1961, **122**, 1414.